



# Fermi National Accelerator Laboratory

FERMILAB-Pub-76/84-EXP  
7100.096

(Submitted to Phys. Rev. Lett.)

INCLUSIVE HADRON SCATTERING FROM 50 TO 175 GeV/c

Fermilab Single Arm Spectrometer Group

October 1976



Inclusive Hadron Scattering from 50 to 175 GeV/c\*

Fermilab Single Arm Spectrometer Group

R. L. Anderson, D. S. Ayres, D. S. Barton, A. E. Brenner, J. Butler,  
D. Cutts, C. DeMarzo, R. Diebold, J. E. Elias, J. Fines, J. I. Friedman,  
B. Gittelman, B. Gottschalk, L. Guerriero, D. Gustavson, H. W. Kendall,  
R. E. Lanou, P. Lavopa, L. J. Levinson, J. Litt, E. Loh, G. Maggi,  
J. T. Massimo, R. Meunier, G. Mikenberg, B. Nelson, F. Posa, K. Rich,  
D. M. Ritson, L. Rosenson, G. Selvaggi, M. Sogard, P. Spinelli,  
R. Verdier, F. Waldner, and G. A. Weitsch

Argonne National Laboratory, Argonne, IL 60439

Universita di Bari and Istituto Nazionale di Fisica Nucleare, Sezione di Bari, Italy

Brown University, Providence, RI 02912

CERN, Geneva, Switzerland

University of Chicago, Enrico Fermi Institute, Chicago, IL 60637

Cornell University, Ithaca, NY 14850

Fermi National Accelerator Laboratory, Batavia, IL 60510

Massachusetts Institute of Technology, Cambridge, MA 02139

Northeastern University, Boston, MA 02115

Stanford Linear Accelerator Center, Stanford, CA 94305

Abstract

This paper reports measurements for the processes  $a + p \rightarrow a + X$  where  $a$  is  $\pi^\pm$ ,  $K^\pm$ ,  $p^\pm$  over a range of Feynman  $x$  from 0.7 to 0.965 at Fermilab energies. The data for all reactions are well represented by a simple parameterization. The cross sections show significant energy dependence in the high  $x$  region. While the data are consistent with factorization in the high  $x$  region and small  $t$ , the proton data are inconsistent with factorization for  $x \leq 0.9$ .

\* Work supported in part by the U.S. Energy Research and Development Administration, the National Science Foundation and INFN (Italy).

We report here measurements of the inclusive reactions  $a + p \rightarrow a + X$  where  $X$  is an undetected missing mass, and  $a$  is one of the six particles  $\pi^\pm$ ,  $K^\pm$ ,  $p$ , or  $\bar{p}$ . This is the first systematic study of these six processes. The measurements were performed at Fermilab, using the Single Arm Spectrometer Facility, at beam momenta of 50, 70, 100, 140, and 175 GeV/c. They cover a range in four-momentum transfer squared  $-t$  of approximately 0.03 to 0.7 GeV<sup>2</sup> and a range in  $x$  from 1.0, the elastic peak, down to approximately 0.75. To good approximation  $x$  is equal in our kinematic region to the Feynman variable and is defined here as

$$x = p_s/p_b \sim 1 - \frac{M_x^2 - m_p^2}{s}, \quad (1)$$

where  $p_b$  and  $p_s$  are the beam and spectrometer momenta respectively.

The quantities  $M_x$ ,  $m_p$  and  $s$  are the missing mass, proton mass and center-of-mass energy squared, respectively. We will not include here any discussion of the resonance region or that part of the nonresonant inelastic spectrum above  $x = 0.975$ . A detailed study of this region will be reported separately.<sup>1</sup>

The experiment was performed simultaneously with a measurement of elastic scattering using the same equipment,<sup>2</sup> and our cross section normalization is obtained from those elastic cross sections. Details of the experimental apparatus will be published elsewhere.<sup>3</sup> A brief description is contained in Ref. 2, and only a few salient details are given here.

Incoming beam particles were provided by the M6E high-resolution beam line, instrumented with Cerenkov counters and hodoscopes so that momenta, angles and particle identification could be recorded. Upstream from the liquid hydrogen target, a magnetic angle-varying system selected the angle of incidence of the incoming beam (and thus determined the scattering angle for particles scattered into the fixed-position spectrometer). Downstream from the target scattered particles were detected by the focusing Single Arm Spectrometer, instrumented with Cerenkov counters, a scintillator hodoscope, and proportional wire chambers. This system measured angles and momenta and provided particle identification. The momentum acceptance of the spectrometer was  $\pm 3\%$  and the scattering angle acceptance was  $\pm 1.5$  mrad. All reactions for a given beam polarity were detected in parallel.

Inelastic cross sections were measured in "sweeps": the beam momentum and spectrometer scattering angle were fixed while the spectrometer momentum was lowered in steps of 5%. Measurements were performed at both positive and negative scattering angles<sup>3</sup> to average out any small angular misalignments between the beam and spectrometer. Elastic scattering runs were made before or after a sweep under identical conditions and were used with our published elastic cross sections<sup>2</sup> to calibrate the acceptance of the spectrometer and detection efficiencies for the conditions of the sweeps. Correction factors for double scattering, radiative corrections,<sup>4</sup> attenuation and decay in flight were applied to obtain the final cross sections. Uncertainty in the elastic scattering cross sections contributed

an overall normalization error of  $\pm 3\%$ . Uncertainties in corrections applied to the elastic peaks also contributed a  $t$ -dependent error ranging from  $\pm 1\%$  at small  $t$  to  $\pm 6\%$  at  $-t \pm 0.8 \text{ GeV}^2$ . Statistical errors associated with these peaks were typically  $\pm (1 \text{ to } 2)\%$  at small  $t$ , increasing to about  $\pm (2 \text{ to } 3)\%$  at  $-t = 0.5 \text{ GeV}^2$ . At  $-t = 0.7 \text{ GeV}^2$  they amounted to typically  $\pm 6\%$ . Nonuniformity of the spectrometer acceptance led to corrections of about  $5\%$  with an associated  $\pm 3\%$  uncertainty in the inclusive cross sections. Corrections for K decay approached  $40\%$ . Double scattering corrections never exceeded  $7\%$  and are believed known to  $\pm 0.5\%$ . The overall errors of the corrections (taken in quadrature) accordingly ranged from about  $\pm 5\%$  at small  $t$  to  $\pm 10\%$  at large  $t$ .

We have compared the absolute values for our proton cross sections at  $175 \text{ GeV}/c$  to those of other experiments in this energy region. We are consistently higher than the USA-USSR<sup>5</sup> and Imperial College-Rutgers<sup>6</sup> internal target experiments by between 1 and 2 standard deviations (we have added their quoted systematic errors linearly to errors determined from their fits to their data). We are higher than, but within a standard deviation of, the Fermilab bubble chamber results at  $205 \text{ GeV}/c$ <sup>7</sup> for values of  $-t$  greater than  $0.1 \text{ GeV}^2$ . Below  $-t = 0.1 \text{ GeV}^2$  the bubble chamber cross sections are considerably lower than ours. We do not regard this as significant, however, since several factors, described in reference 7, conspire to reduce the bubble chamber cross sections in this region. Our results extrapolate quite well to ISR data.<sup>8</sup>

The considerable amount of data collected in this experiment could all be fitted by an empirical form for the invariant cross section,

$$s \frac{d^2 \sigma}{dtdM_x^2} = A_1(s, t)(1 - x) + A_2(s, t)/(1 - x). \quad (2)$$

No obvious theoretical justification for this simple expression exists, although the two terms might be expected to approximately simulate the behavior of Reggeon and Pomeron exchanges.

Figure 1 shows the invariant cross section  $sd^2\sigma/dtdM_x^2$  versus  $x$  at constant  $t$  for the six incident particles. At high  $x$  the so-called diffractive peak region, corresponding to the  $A_2$  term of Eq. (2), is evident.

Table I tabulates best fit values of  $A_1(s, t)$  and  $A_2(s, t)$  in the form  $A(s, t) = Ae^{Bt + Ct^2} \cdot (1 + D(E^{-\frac{1}{2}} - 0.1))$ , where  $E$  is the laboratory energy of the beam particle in GeV.  $A_2(s, t)$  is approximately represented by a simple exponential whereas the  $A_1(s, t)$  term shows a strong change of slope associated with a large  $C$  coefficient. The data are well represented by the fits, with deviations generally less than 10%.

The parameters  $D_2$  in Table I indicate a significant energy dependence in the high  $x$  region where the term  $A_2$  dominates. The proton cross section decreases by 17% over our energy range, and the pions by about 21%. Kaons and the antiprotons show a decrease of 30% to 40%. Away from the high  $x$  region, however, all particles show essentially no energy dependence. There is evidence in the proton and  $\pi^\pm$  data that the coefficient  $D_2$  has a  $t$  dependence. The proton cross sections change by 12, 19, and 26%, respectively, for  $-t$  in the ranges 0-0.2, 0.2-0.4, 0.4-0.6  $\text{GeV}^2$ . No other systematic deviations from the fit are seen.

In a simple Regge model where a single trajectory dominates both the elastic and inelastic cross sections, the ratio of the inelastic to the elastic cross section at the same value of  $t$  should be independent of the beam particle. This statement of factorization should be correct for  $x$  values close to 1, and at high energy where the cross sections should be dominated by a Pomeron coupling to the beam-particle - spectrometer-particle vertex; it may fail for lower  $x$  values where various Reggeon exchanges are possible. Factorization is indeed satisfied for the  $\pi^+$  and proton to about  $\pm(5$  to  $10)\%$  for  $x$  near 1 and  $-t \leq 0.4 \text{ GeV}^2$ . The  $\pi^+$  inelastic/elastic ratio decreases relative to the proton as  $t$  increases and as  $x$  decreases, reaching about 30% at  $x = 0.75$  and  $-t = 0.4 \text{ GeV}^2$ . While the  $K^+$  ratio also decreases relative to the proton as  $x$  decreases, the  $K^+$  and  $\pi^+$  ratios follow one another to about  $\pm 20\%$  over our entire kinematic range. The antiparticles exhibit qualitatively similar behavior.

The severe departure from factorization associated with protons as  $x$  decreases suggests the presence of an additional effect not present in the  $\pi$  or  $K$  reactions. Within the triple Regge formalism a possible candidate is the  $\pi\pi P$  term<sup>9</sup> which is allowed only in proton (and  $\bar{p}$ ) reactions and yields a rise in the proton cross section for  $x \leq 0.9$  as shown in Fig. 1b (and Fig. 1e). However, the increase in the proton cross section in this region relative to that for  $\pi$  or  $K$  may also be partly attributed to decay products of nucleon isobars from the diffractive peak. Simple kinematic arguments suggest that such a mechanism in  $\pi$  or  $K$  reactions in this  $x$  region would have much less effect than for protons.

We thank the staff of Fermilab, and especially of the Meson Laboratory for their assistance in the construction of the Single Arm Spectrometer facility and in the execution of this experiment. The member institutions of this collaboration gratefully acknowledge the assistance of their support staffs.

#### REFERENCES

1. Fermilab Single Arm Spectrometer Group, "Inelastic Diffractive Scattering at Fermilab Energies", to be published.
2. Fermilab Single Arm Spectrometer Group, Phys. Rev. Letters 35, 1195 (1975).
3. Fermilab Single Arm Spectrometer Group, " $\pi^\pm p$ ,  $K^\pm p$ ,  $pp$  and  $\bar{p}p$  Elastic Scattering from 50 to 175 GeV/c", submitted to Phys. Rev. D.
4. M. R. Sogard, Phys. Rev. D9, 1486 (1974), and D11, 183 (1975).
5. Y. Akimov et al., Phys. Rev. Letters 35, 766 (1975).
6. K. Abe et al., Phys. Rev. Letters 31, 1527 (1973).
7. J. Whitmore et al., Phys. Rev. D11, 3124 (1975).
8. M. G. Albrow et al., "Inelastic Diffractive Scattering at the CERN ISR", CHLM Collaboration preprint, 1976 (unpublished).
9. M. Bishari, Phys. Letters 38B, 510 (1972).

Table I. Results of global fits to the data on each particle for the parameterization

$$s \frac{d^2\sigma}{dt dM^2} = A_1 e^{B_1 t + C_1 t^2} \left[ 1 + D_1 (E^{-1/2} - 0.1) \right] (1-x) + A_2 e^{B_2 t + C_2 t^2} \left[ 1 + D_2 (E^{-1/2} - 0.1) \right] \left( \frac{1}{1-x} \right),$$

where E is the incident laboratory beam energy. Errors are statistical plus systematic folded in together.

Channel	$A_1$ (mb/GeV <sup>2</sup> )	$B_1$ GeV <sup>-2</sup>	$C_1$ GeV <sup>-4</sup>	$D_1$ GeV <sup>1/2</sup>	$A_2$ (mb/GeV <sup>2</sup> )	$B_2$ GeV <sup>-2</sup>	$C_2$ GeV <sup>-4</sup>	$D_2$ GeV <sup>1/2</sup>
$\pi^+$	113 ± 7	8.00 ± 0.30	6.21 ± 0.50	-0.68 ± 0.60	2.30 ± 0.12	5.21 ± 0.15	1.72 ± 0.20	3.64 ± 0.40
$\pi^-$	120 ± 7	7.76 ± 0.32	5.33 ± 0.50	1.15 ± 1.00	2.50 ± 0.14	5.04 ± 0.16	1.20 ± 0.22	3.39 ± 0.46
$P^+$	612 ± 30	8.32 ± 0.16	5.24 ± 0.24	-0.28 ± 0.40	6.08 ± 0.36	7.24 ± 0.14	2.58 ± 0.22	2.69 ± 0.28
$P^-$	609 ± 50	8.42 ± 0.50	6.25 ± 0.80	-2.15 ± 1.50	6.09 ± 0.70	6.53 ± 0.60	-0.66 ± 1.50	8.16 ± 2.00
$K^+$	69 ± 8	7.66 ± 0.80	6.85 ± 1.00	-1.29 ± 1.73	1.30 ± 0.10	3.64 ± 0.32	0.83 ± 0.44	5.51 ± 2.00
$K^-$	65 ± 14	7.75 ± 1.30	5.90 ± 1.50	-3.81 ± 4.00	1.56 ± 0.14	3.85 ± 0.40	0.64 ± 0.60	7.31 ± 2.50

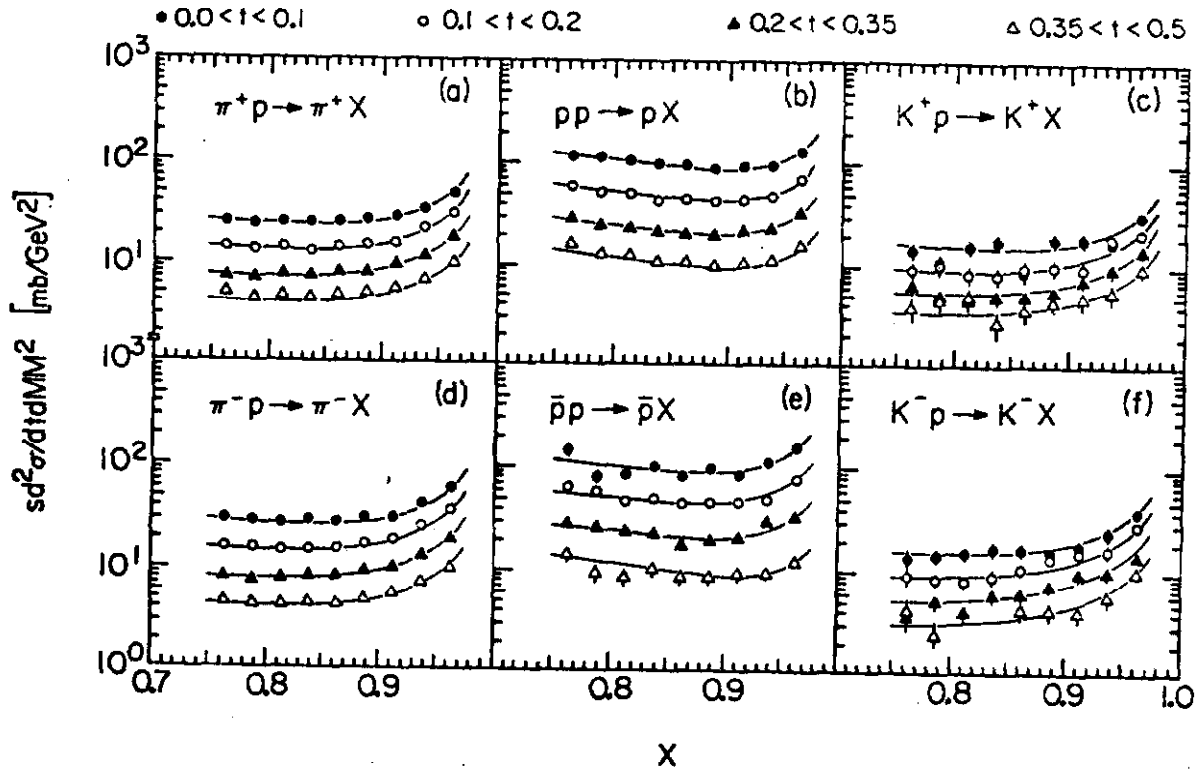


Fig. 1 Inclusive cross sections at 70 GeV/c incident momentum for the ranges of momentum transfer indicated. The curves show the results of the fits in Table I.